Cavity Formation and Light Propagation in Partially Ordered and Completely Random One-Dimensional Systems

Shih-Hui Chang, Hui Cao, and Seong Tiong Ho, *Member, IEEE*

Abstract—We study light transport in ordered, partially ordered, and completely random one-dimensional (1-D) systems. In a periodic structure, there are three types of passbands with different origins. When disorder is introduced to a periodic system, the passbands change differently, depending on their origins. The transmissivity and decay length in the passbands near the band edges decrease drastically. The stopbands are widened. The introduction of randomness to a periodic structure enhances light localization in frequency regions in which it is delocalized in a periodic structure. In a completely random system, a resonant cavity is formed by two stacks of multiple layers which serve as two highly reflective broadband mirrors. We calculate the size and the quality factor of 1-D random cavities. With an increase in the degree of disorder, the lasing threshold in such a cavity first decreases, then increases. The lasing frequency spreads from the band edge toward the stopband center.

Index Terms—Cavity resonator, electromagnetic propagation in random media, electromagnetic scattering by periodic structure, electromagnetic scattering by random media, random laser, random media.

I. INTRODUCTION

THE RECENT discovery of a random laser [1]–[3], a laser made of a random medium, has received considerable interest. Random media, i.e., dielectric media with a random spatial variation of the refractive index, can confine light in a very small region. It is possible to make a laser in such a random medium that does not require a pre-defined physical cavity. To better understand the phenomenon and further investigate how the cavity is formed, we conduct a systematic study of the impact of the material and geometric properties of a random medium on the performance of random lasers.

In contrast to a periodic dielectric structure is a system where the dielectric particles are randomly distributed. The interference of scattered light ultimately leads to light localization [4], [5]. Therefore, light propagation can be inhibited in a disordered system [6], [7]. To achieve light localization in a three-dimensional (3-D) disordered system, the Ioffe–Regel criterion should be satisfied: $kl < 1$, where k is the wavevector and

l is the transport mean free path. John first suggested that the Ioffe–Regel criterion could be more easily met in photonic crystals with some disorder [8]. The density of states is nearly zero near the band edges. When the frequency of the light is near a photonic band edge, the Ioffe–Regel criterion is replaced by $k_{\text{cryst}}l < 1$, where k_{cryst} is the "crystal momentum" and is much smaller than k. Therefore, introducing some order to a disordered system helps light localization.

Light transport in a disordered medium is closely related to that in an ordered medium. In this paper, we study how the light transport behavior evolves when a one-dimensional (1-D) system changes continuously from a perfectly ordered structure to a highly disordered structure. Specifically, we calculate the transmissivity, decay length and mode linewidth in 1-D systems that are ordered, partially ordered, and highly disordered.

There have been many theoretical studies of periodic-on-average 1-D systems [9]–[14]. However, most studies were limited to the case of weak disorder and the interplay of the photonic bandgap (PBG) and light localization was not emphasized. In this paper, we focus on the effect of the PBG on a random medium. We start with an ordered array of particles having the same diameter. Then we either keep the particle diameter constant and randomize the distance between particles, or randomize the particle diameter and keep the distance between particles constant. Both cases belong to partially ordered systems. Finally, we randomize both the particle diameter and the distance between particles to obtain fully disordered structures.

In our study of the optical properties of 1-D dielectric media which transit from an ordered distribution to a disordered distribution, we found that the transmissivity and decay length near the passband edges are very sensitive to disorder. With the introduction of disorder to a periodic structure, the transmissivity and decay length in the passbands near the band edges decreases drastically. The stopbands are widened. Therefore, the introduction of randomness to a periodic structure enhances light localization in frequency regions in which it is delocalized in a periodic structure. In the highly disordered cases, the partially random system shows the remnant resonant peaks in the transmission spectrum due to the fixed particle size or gap size. The complete random system shows uniform transmission across the entire frequency region except the long-wavelength limit.

We study how resonant cavities are formed in 1-D random media and what parameters affect the properties of these random cavities (such as cavity size and lifetime). For the completely

S.-H. Chang and S. T. Ho are with the Department of Electrical and Computer Engineering, Northwestern University, Evanston IL 60208 USA (e-mail: s-chang4@nwu.edu).

H. Cao is with the Department of Physics and Astronomy, Northwestern University, Evanston, IL 60208 USA.

random system, we calculate the localization length of light and the statistics of the resonant mode linewidth in each individual sample.

This paper is organized as follows. Section II describes the random structures and the method of our calculation. In Sections III–V, we discuss the effect of disorder on the PBG and its optical properties in media which transit from order to disorder. Specifically, Section III is a brief review of PBG physics. Section IV is a study of partially ordered 1-D systems. Section V discusses completely random 1-D systems. In Section VI, we study the formation and size of resonant cavities in random media. In Section VII, we study the linewidth of random cavity modes and their statistics in the random system. Finally, in Section VIII, we present our conclusions.

II. MODEL OF RANDOM MEDIA

In this paper, our 1-D random medium model is comprised of dielectric slabs in air having random thickness a and spacing b. Here, a slab is a 1-D representation of a particle. a and b have the mean values a_0 and b_0, respectively. We assume $a = a_0(1+2\sigma_a r)$ and $b = b_0(1+2\sigma_b r)$, where r is a random number distributed uniformly between -0.5 and 0.5, $0 \leq \sigma_a$ and $\sigma_b \leq 1$ give the amplitude of randomness, and n_a (n_b) is the refractive index of the dielectric slabs (air).

For a periodic system, $\sigma_a = \sigma_b = 0$. There are two types of partially ordered systems.

1) Random spacing, where the particle size is uniform, but the spacing between particles is random. Here $\sigma_a = 0$, $\sigma_b > 0$.
2) Random particle size, where the particle size is randomized, while the spacing between particles remains constant. Here $\sigma_a > 0$ and $\sigma_b = 0$.

Both systems are partially random systems, because some parameter is kept constant. For a completely random system, both the particle size and the spacing between particles are random. Here, $\sigma_a > 0$ and $\sigma_b > 0$.

The ratio of the average particle size a_0 to the average spacing b_0 gives the filling factor of the system. As the filling factor increases, the medium becomes more compact. We further divide random media into three categories in terms of the compactness: 1) Dense ($n_a a_0 / n_b b_0 \gg 1$), where the majority is dielectric material; 2) loose ($n_a a_0 / n_b b_0 \ll 1$), where the majority is air; and 3) half-filled ($n_a a_0 / n_b b_0 \sim 1$), where the optical path lengths in particles and air gaps are about the same.

We use the transfer matrix method to calculate optical transmission through a 1-D system [15]. The typical transmission spectrum for a specific random structure consists of many resonant peaks. Those peaks are washed out after the transmission spectra are averaged over an ensemble of random structures. The transmission spectra that we present in this paper are averaged over 1000 random structures. We numerically find that averaging over 1000 realizations of the random structure is enough to obtain the ensemble-averaged values. The ensemble average gives some general characteristics of the random dielectric media. However, we would like to point out that in the study of the physical phenomena on which the fine features specific
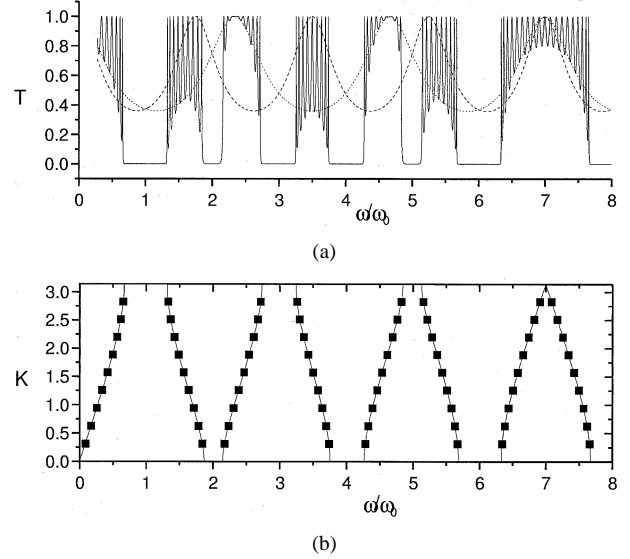

Fig. 1. (a) Transmission spectrum plot. Solid line: the ten unit cells with cell size $\Lambda = a + b$, $a = 100$ nm, $b = 400$ nm, $n_a = 3$, $n_b = 1$, where $\omega_0 = 2\pi c / 2(n_a a + n_b b)$. Dotted line: the single dielectric layer $a = 100$ nm $n_a = 3$. Dashed line: the single gap layer $b = 400$ nm, $n_b = 1$. The resonant peaks of single dielectric or gap layer overlap with the passband of the ten-unit cell. This indicates there are two types of passband: the dielectric band and the air band. When the two bands coincide, we call it a combined band. (b) Dispersion relation $K - \omega$ of periodic structure. The 19 ($= 2N - 1$) dots indicate the resonant modes of the ten-unit cell. The frequency of the resonant mode was modified by the dispersion curve.

to individual structures have a significant effect, the ensemble average should not be applied.

III. PERIODIC STRUCTURE

Light transport in 1-D periodic structures has been extensively studied and well understood. Standard treatment can be found in [15] and [16] and the main results in [16]–[18]. To compare with random structures in later sections, we will summarize the important aspect of periodic structures obtained by standard transfer matrix method.

A 1-D periodic structure of interest here is made of alternating dielectric layers A and B. In the following discussion, layer A has a refractive index $n_a = 3$ and a thickness $a = 100$ nm. Layer B has a refractive index $n_b = 1$ and a thickness $b = 400$ nm. We define a unit cell as one pair of layer A and layer B. The optical path length through a unit cell is $l_{\text{uc}} = (n_a a + n_b b)$. The fundamental resonant frequency for a unit cell is $\omega_0 = 2\pi/\lambda_0$, where $\omega_0 = 2l_{\text{uc}}$ is equal to the round-trip optical length in the unit cell.

Fig. 1(a) plots the transmission spectrum when the number of dielectric slabs N is equal to ten. The frequency ω is normalized to ω_0. The frequency regimes with nearly zero transmissivity represent the stopbands for light propagation. The center frequencies of the stopbands are denoted by $\omega_m = m\omega_0$, where m is a positive integer. The spectral width of the stopbands is proportional to the contrast of the refractive indices, indicated by $(n_a - n_b)/(n_a + n_b)$. Between two adjacent stopbands are the passbands. There are two sets of passbands. One set is called particle-related passbands, which are centered on the resonant frequencies of a single particle $m\omega_a$, where $\omega_a = 2\pi c/2n_a a$.
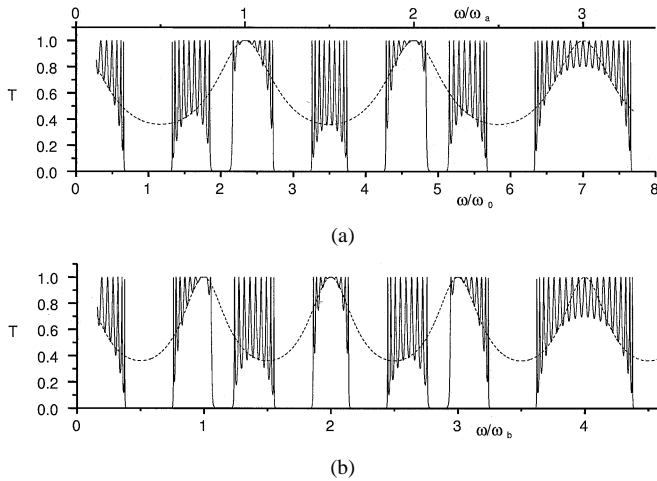
Fig. 2. (a) Transmission spectrum of ten-unit cells ended with air (solid line) and single dielectric layer (dash line). The resonant peak in the overlapped dielectric-like passband is modified by the resonant effect of the single dielectric layer. $\omega_0 = 2\pi c/2(n_a a + n_b)$, $\omega_a = 2\pi c/2n_a a$, $a = 100$ nm, $b = 400$ nm, $n_a = 3$, $n_b = 1$. (b) Transmission spectrum of ten-unit cell ended with dielectric materials (solid line) and single gap layer (dash line). The resonant peaks in the overlapped gap-like passband are modified by the resonant effect of the single air gap layer. $\omega_b = 2\pi c/2n_b b$.
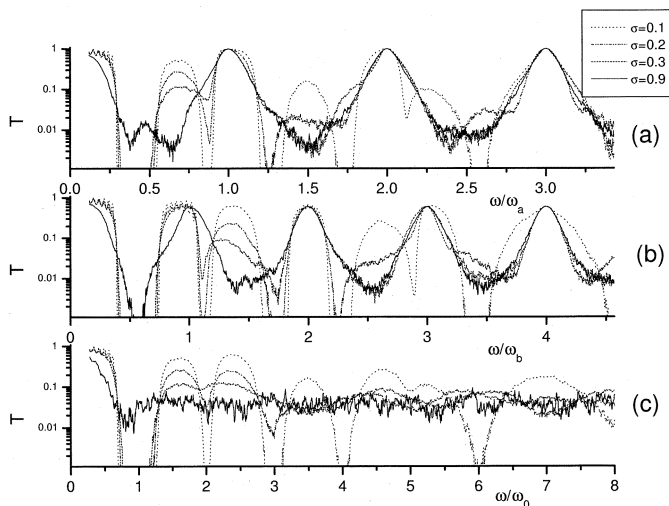

Fig. 3. Ensemble averaged transmission spectrum plots. (a) Partial random system of type I, random gap thickness b, fixed dielectric layer thickness a_0. There are ten layers in the system with averaged gap size $\bar{b} = b_0$. (b) Partial random system of type II, random dielectric layer thickness a, fixed gap thickness b_0. There are ten layers in the system with averaged dielectric thickness $\bar{a} = a_0$. (c) Complete random system, random dielectric layer thickness a, random gap thickness b. There are ten layers in the system with averaged $\bar{a} = a_0$ and $\bar{b} = b_0$. Here, the a_0, b_0, n_a, n_b parameters are the same as the Fig. 2 periodic system.

The other set is called gap-related passbands, which are centered on the resonant frequencies of a single air gap $m\omega_b$, where $\omega_b = 2\pi c/2n_b b$. Within a particle-related passbands, the light field is concentrated inside the particles. Within the gap-related passbands, the light field is concentrated inside the air gaps. As shown in Fig. 1(a), some stopbands are closed and two adjacent passbands of different types merge. We call such a passband a combined passband. It occurs at the frequency that is a common multiple of ω_0, ω_a, and ω_b. With the parameters, we use $(n_a a/n_b b = 3/4)$, the lowest order combined passband centers at $7\omega_0$ ($= 3\omega_a = 4\omega_b$).

Fig. 1(b) shows the dispersion relation for the lowest seven passbands of the periodic structure. The transmission eigenmodes (TEMs) of an $N = 10$ sample, plotted as black dots, correspond to the resonant peaks of the passbands in the transmission spectrum. The number of transmission eigenmodes within a particle-related or gap-related passband is equal to $N - 1$. A combined passband has $2N - 1$ modes. These transmission eigenmodes are not equally spaced in frequency. Toward the edges of the passbands, the transmission eigenmodes get closer to each other. The spectral linewidth of the TEM near the passband edges is smaller than that of the TEM near the passband center. The envelope function for the TEM closest to the edge of a passband has only one maximum. The second closest TEM has two intensity maxima. As the frequency of a TEM moves closer to the center frequency of a passband, its intensity tends to distribute more evenly across the entire medium.

As shown in Fig. 2(a), the transmission peaks in the particle-related passbands are less pronounced than those in the gap-related passbands. This is caused by the boundary effect. The periodic structure is surrounded by air. The transmissivity in the particle-related passbands is modified by the transmissivity through a single particle. Fig. 2(b) shows the transmission spectrum when the periodic structure is surrounded by the dielectric material of refractive index n_a. The transmissivity of the gap-related passbands is modified by the transmissivity of a single air gap surrounded by the dielectric material. Thus, the transmission peaks in the gap-related passbands become less pronounced.

Even though light within a stopband hardly transmits through a periodic structure, it penetrates into the structure. The penetration depth is characterized by the decay length [19], [20]. It is defined as the distance over which the light intensity is reduced to $1/e$ of its input value. The decay length is the shortest at the center of the stopbands. As the frequency approaches the edges of the stopbands, the decay length increases. With the refractive index ratio $n_a/n_b = 3$, the decay length in $\sim 80\%$ of the stopbands is shorter than the period of the structure. Our calculation shows that the decay length decreases as the filling factor increases.

IV. PARTIALLY ORDERED SYSTEM

In this section, we will study two partially ordered 1-D systems. In the first, the spacing between particles is randomized, while the particle size is kept constant. Namely, $a = a_0 = 400$ nm, $b = b_0(1 + 2\sigma_b r)$, $b_0 = 100$ nm, $r = (-0.5, 0.5)$ with a uniform distribution. Fig. 3(a) shows the transmission spectra with various degrees of randomness σ_b. The frequency ω is normalized to ω_a. The introduction of randomness to a perfectly ordered structure decreases the transmissivity in the passbands drastically and increases the transmissivity in the stopbands slightly. As a result, the stopbands are widened. The transmission peaks in the passbands disappear after ensemble averaging. The randomization of the air gap thickness eventually removes the gap-related passbands. However, the particle-related passbands survive, even in the presence of a large degree of disorder (e.g., $\sigma_b = 0.9$). Their spectral width decreases but eventually saturates to a finite
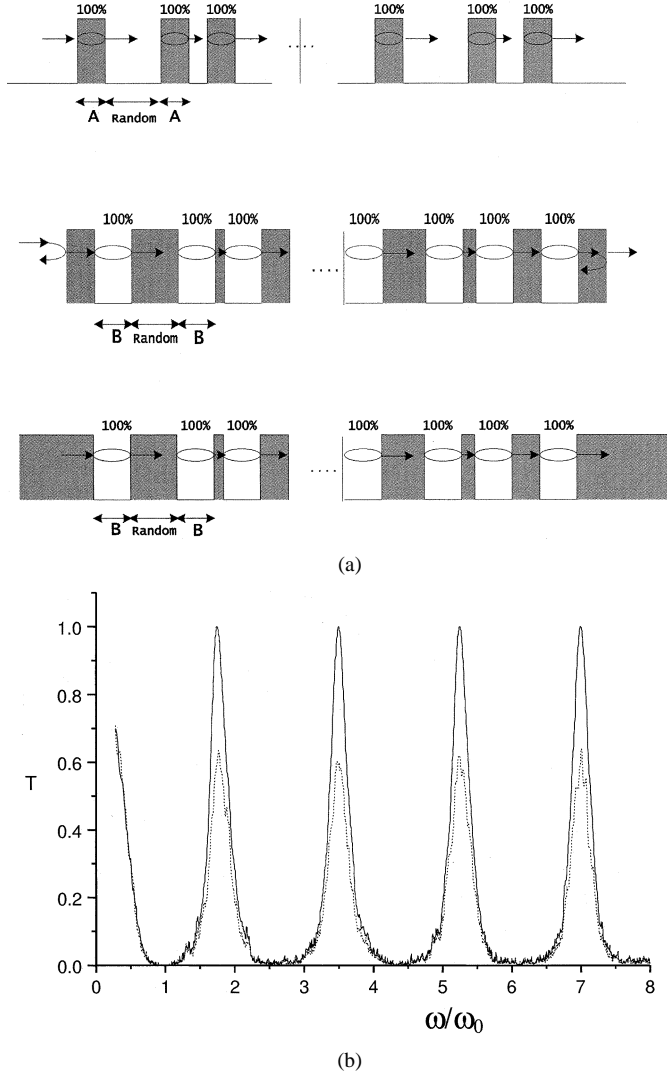
(a)

(b)

Fig. 4. (a) Schematic diagram of the resonant transmission in the partial random system. Top: type I, random gap layer with fixed dielectric thickness. The transmissivity is 100% in the resonant mode. Middle: type II, random dielectric layer with fixed gap thickness. The transmitivity is smaller than 1 due to the reflection from the end boundary. Bottom: type II embedded in dielectric materials. There is 100% transmissivity in the resonant mode. (b) Plot of the ensemble averaged transmission spectrum of partial random system of type II with 90% randomness with ten layers in the system. Dashed line: the sample embedded in the air. Solid line: the sample embedded in the dielectric materials.

value. The maximum transmissivity within a particle-related passband remains unity. Our calculation shows that the ensemble-averaged transmissivity of a particle-related passband approaches t_s^N as σ_b increases, where t_s is the transmissivity of a single particle. Therefore, the partially ordered system behaves like N independent filters in series without multiple interference among them. At the resonant frequencies of a single particle surrounded by air, the transmissivity through a single particle is also unity. As illustrated in the top diagram of Fig. 4(a), when the light transmits 100% through one particle due to Fabry–Perot resonance, it also transmits 100% through the next particle, which has the same size and resonance as the first one. Thus, the transmissivity through the entire structure is unity, regardless of the degree of disorder in the particle spacing.

Next, we randomize the particle size but keep the particle spacing constant. Namely, $a = a_0(1 + 2\sigma_a r)$, $a_0 = 300$ nm, $b = b_0 = 400$ nm. Similar behavior is found in the transmission spectra shown in Fig. 3(b). The frequency ω is normalized to ω_b. As σ_a increases, the particle-related passbands diminish and eventually disappear. However, the gap-related passbands survive due to the constant spacing between particles. The maximum transmissivity in a gap-related passband decreases slightly from unity. As illustrated in the middle diagram of Fig. 4(a), the decrease results from the reflections at the two boundaries of the system. Because the partially ordered system is surrounded by air, the transmissivity of a gap-related passband is equal to the product of $N-1$ multiples of the transmissivity of an air gap and the transmissivity of two surfaces. If the sample is surrounded by the dielectric material with refractive index n_a instead of air, as illustrated in the bottom diagram of Fig. 4(a), the maximum transmissivity of the gap-related passbands remains unity, regardless of the degree of disorder σ_a Fig. 4(b).

In the above two types of partially ordered systems, the combined passbands always remain. When the particle size is randomized, light in the combined passbands can still transmit through the system due to the resonant effect of the air gaps with constant thickness. When the particle spacing is randomized, the resonant transmission through the particles of uniform size keeps the combined passbands remaining.

As a partially ordered structure gets bigger (the number of dielectric layers N increases), the spectral width of the remaining passbands decreases. This can be explained by the effect of multiple filtering. As the number of filters increases, the passbands become narrower.

V. COMPLETELY RANDOM SYSTEM

From the above results for partially ordered 1-D systems, we realize that in order to have a completely random 1-D system, we must randomize both the particle size and spacing. In the present case, $a = a_0(1+2\sigma_a r)$, $a_0 = 400$ nm. $b = b_0(1+2\sigma_b r)$, and $b_0 = 100$ nm. For simplicity, we set $\sigma_a = \sigma_b$ in our calculation. Fig. 3(c) plots the transmission spectrum of a completely random system. Unlike a partially ordered system, all passbands diminish and eventually disappear as the degree of the randomness σ $(= \sigma_a = \sigma_b)$ increases. Higher order passbands are more sensitive to disorder. The transmissivity of higher order passbands decreases more rapidly when randomness is introduced. The transmissivity in the stopbands increases slightly as the randomness increases. In the presence of large randomness, the band structures in the transmission spectrum disappear, and the transmissivity is nearly zero everywhere except in the zeroth-order passband. The wavelength of light in the zeroth–order passband is much larger than the particle size, so that light simply passes through the medium without much scattering. In this limit, the media behaves as if it is homogeneous. Therefore, the transmissivity in the zeroth-order passband remains high. Since all the light with frequency above the edge of the zeroth-order passband is reflected, a completely random medium behaves like a wideband mirror.

Next, we calculate the decay length in a completely random system. The decay length is an important parameter for light lo-
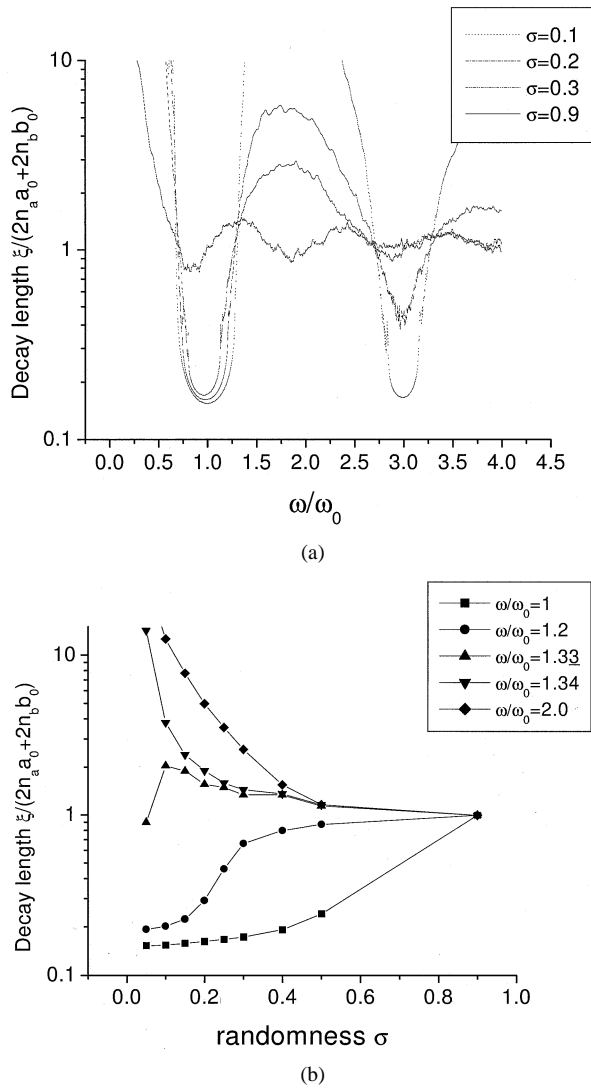
Fig. 5. (a) Ensemble averaged decay length versus frequency ω for different degree of randomness ($\sigma = 10\%$, 20%, 30%, 90%) in the type of complete random system with ten layers $\omega_0 = 2\pi c/2(n_a a + n_b)$, $a = 100$ nm, $b = 300$ nm $n_a = 3$, $n_b = 1$. (b) Ensemble averaged decay length versus randomness σ at different bands for a complete random system with ten layers. $\omega/\omega_0 = 1.0$ (forbidden gap center), $\omega/\omega_0 = 1.2$ (forbidden gap), $\omega/\omega_0 = 1.33$ (bandgap edge), $\omega/\omega_0 = 1.34$ (slightly above bandgap edge), $\omega/\omega_0 = 2.0$.

calization. Here, we set $a_0 = 100$ nm, $b_0 = 300$ nm. Since $n_a a_0 = n_b b_0$, we have $\omega_a = \omega_b$. Thus, all the passbands are combined passbands. Fig. 5(a) plots the decay length as a function of frequency for various degree of randomness σ. As σ increases, the decay length in the passbands decreases, while the decay length in the stopbands slightly increases. In the case of large randomness, the decay length is nearly constant in the entire frequency regime except the zeroth-order passband. To illustrate this result more clearly, we plot in Fig. 5(b) the decay length as a function of σ. The decay length is calculated at the following frequencies: $\omega = \omega_0$ (at the center of the first stopband), $\omega = 1.2\,\omega_0$ (in between the center and edge of the first stopband), $\omega = 1.33\,\omega_0$ (at the edge of the first stopband), $\omega = 1.34\,\omega_0$ (slightly above the edge of the first stopband, inside the first passband), and $\omega = 2.0\,\omega_0$ (at the center of the first passband). As σ increases, the decay length in the passband de-

creases, while the decay length in the stopband increases. Right at the band edge, the decay length does not change much as σ varies. When σ reaches 0.9, the decay length shows no frequency dependence.

The above results are obtained for the half-filled medium ($n_a a_0 = n_b b_0$). Next, we increase the filling factor of the random medium, while keeping the randomness of the particle size equal to that of the particle spacing ($\sigma_a = \sigma_b$). Because the refractive index of the particles is larger than the refractive index of the air gap, the fluctuation of the optical path length in the particles ($n_a \sigma_a$) is larger than that in the air gaps ($n_b \sigma_b$). The dense medium has more particles; thus, its overall randomness is larger than that of a loose medium, and the decay length decreases with an increase of the filling factor.

When the randomness is introduced to a periodic structure, some modes appear in the stopbands. They open up the channels for light propagation through the system. The frequencies of the modes depend on the random structures [21]–[23]. In different random structures, the modes have different frequencies. After ensemble averaging, discrete modes disappear. However, the transmissivity in the stopbands increases, as does the decay length. In the presence of small randomness, the modes in the stopbands are close to the band edges. Thus, only the decay length near the stopband edges increases. When the amplitude of randomness becomes larger, more modes appear in the stopbands and the frequency approaches the central frequencies of the stopbands. As a result, the decay length close to the center of the stopbands starts to increase.

In a periodic structure, the modes in the passbands are formed by constructive interference in the forward direction. When disorder is introduced to the system, the constructive interference is destroyed and the modes in the passbands diminish. Hence, the transmissivity decreases, so does the decay length. The modes closer to the passband edges are more sensitive to the disorder. In the presence of disorder, the modes closer to the passband edges diminish quickly, while the modes near the center of the passbands are less affected. Therefore, the decay length near the passband edges drops quickly with the increase of randomness. In the higher order passbands, the decrease of decay length is even faster. This is because passbands with higher order resonance are more sensitive to disorder.

VI. RANDOM CAVITY SIZE

In a conventional laser, a laser cavity is formed by two highly reflective mirrors, as illustrated in Fig. 6(a). Light bounces back and forth between them. In the case of 1-D random media, a cavity can be formed by distributed feedback of light from two separate spatial regions. The introduction of defects or disorder in a random medium will increase the probability of forming a resonant cavity. How is a cavity formed in such random media with many random defects? How large is the cavity and how good is the cavity? These questions will be answered in this and the following sections.

In a random system, light can experience significant reflection from multiple dielectric layers of random thickness due to wave interference effects. As shown schematically in Fig. 6(b), a random cavity is formed by two stacks (the right-hand side
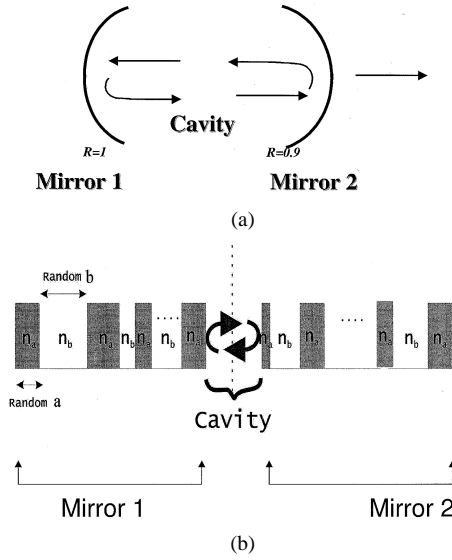
Fig. 6. Resonant mode of laser cavity (a) Conventional lasers. (b) Random media.

and the left-hand side) of multiple layers of random thickness and spacing, which serve as two highly reflective mirrors.

The number of disordered layers needed to form mirrors of high reflectivity will determine how large the random cavity size is. Light inside the random cavity penetrates into the mirrors on both sides for a certain distance. The penetration length is defined as the distance over which the light intensity decays to $1/e$ of that of the incident light. This is also called the decay length. The decay length is a measure of how far the photons travel into the media. When the scattering is strong, light cannot propagate far and has a short decay length. In other words, the decay length is an indication of the strength of photon trapping. The decay length determines the number of random layers needed to form mirrors of high reflectivity and also the size of the resonant cavity mode in the random medium.

The ensemble-averaged transmissivity decays exponentially with the sample length. We can extract the decay length by curve-fitting the transmission with the exponentially decay function of distance $I(x) = I_0 e^{-x/\xi}$, where ξ is the decay length. In our calculations, we obtain transmission as a function of medium length. The transmissivity is ensemble averaged over 1000 samples.

The decay length versus frequency of the completely random 1-D system with refractive index ratio $n_a a_0 : n_b b_0 = 1 : 1$ is plotted in Fig. 5(a). Different lines indicate different degrees of randomness of the system. When the randomness is small, the stopband and passband regions can be clearly distinguished. The decay length in the stopband region is much smaller than that in the passband region. As the randomness increases, the decay length in the passband decreases. Photons in this frequency region are less likely to travel far. They are more likely to be trapped in the random medium. While in the stopband, the decay length increases as the randomness of the system increases. This is because the introduction of disorder in the system reduces the coherent interference. However, the decay length is still relatively small compared with that in the passband region. When the randomness is large $\sigma = 0.9$, the decay length is almost flat

over the entire frequency regime except in the first stopband. The decay length is on the order of one wavelength.

Complete light localization occurs if photons always return to the point of origin. The degree of light localization depends on the sample length. In a 1-D structure, there are only two escape channels for the scattered light, forward or backward. As long as the sample size is much larger than the decay length, light will most likely return to the original point. Therefore, for 1-D random media, strong light localization occurs when the sample size is larger than the decay length.

To reduce the photon localization length and random cavity size, we can either use a dense medium or increase the refractive index of the system. For practical applications, it is important to find the optimal operation region that has strong confinement and low lasing threshold. It is also important to know what system parameters will affect the localization length and the cavity size. We will study the 1-D disordered system with different filling factor and different refractive index.

The localization length for random systems of different filling factor is plotted in Fig. 7(a). The filling factor is defined as $n_a a_0 / (n_a a_0 + n_b b_0)$. This definition of the filling factor gives the portion of the optical path in the particles versus the entire sample. The plot shows that the localization length will approach a constant value at short wavelength. When the wavelength is much shorter than the gap distance, the minimum scattering length is the averaged inter-particle distance.

The normalized localization length (localization length/wavelength) is plotted in Fig. 7(b). This ratio indicates the degree of photon localization. For samples of a different filling factor, the minimum ratio of localization length to wavelength occurs at different frequency. When the filling factor is 1:1, the minimum ratio of localization length over wavelength occurs near the center of the first stopband. This is because the interference effects between the particles and within the particles coincide at this frequency.

Fig. 7(c) shows that the minimum localization length occurs at the first stopband when the filling factor is 1:1. As the filling factor deviates from the 1:1 ratio, the minimum localization occurs at higher frequency region.

In Fig. 8, we plot the localization length for systems with different refractive index contrast. The localization length is normalized to the wavelength. In this plot, the minimum localization length is about λ for the case of $n = 2.2$. As the refractive index increases, the normalized localization length decreases and vice versa.

VII. CAVITY QUALITY FACTOR AND LASING THRESHOLD

In a 1-D random system, the bandgap effect persists in the presence of weak disorder. When the randomness is small, the decay length is short in the stopband. Because the density of states is very low in the stopband, it is most likely to find the cavity modes near the band edge. On the other hand, when the randomness is large, the density of states increases in the stopband, but the decay length in the stopband also increases. It is more likely to have modes in the stopband.

Furthermore, experimental measurement of random lasing is carried out in a single sample. Its behavior is different from the
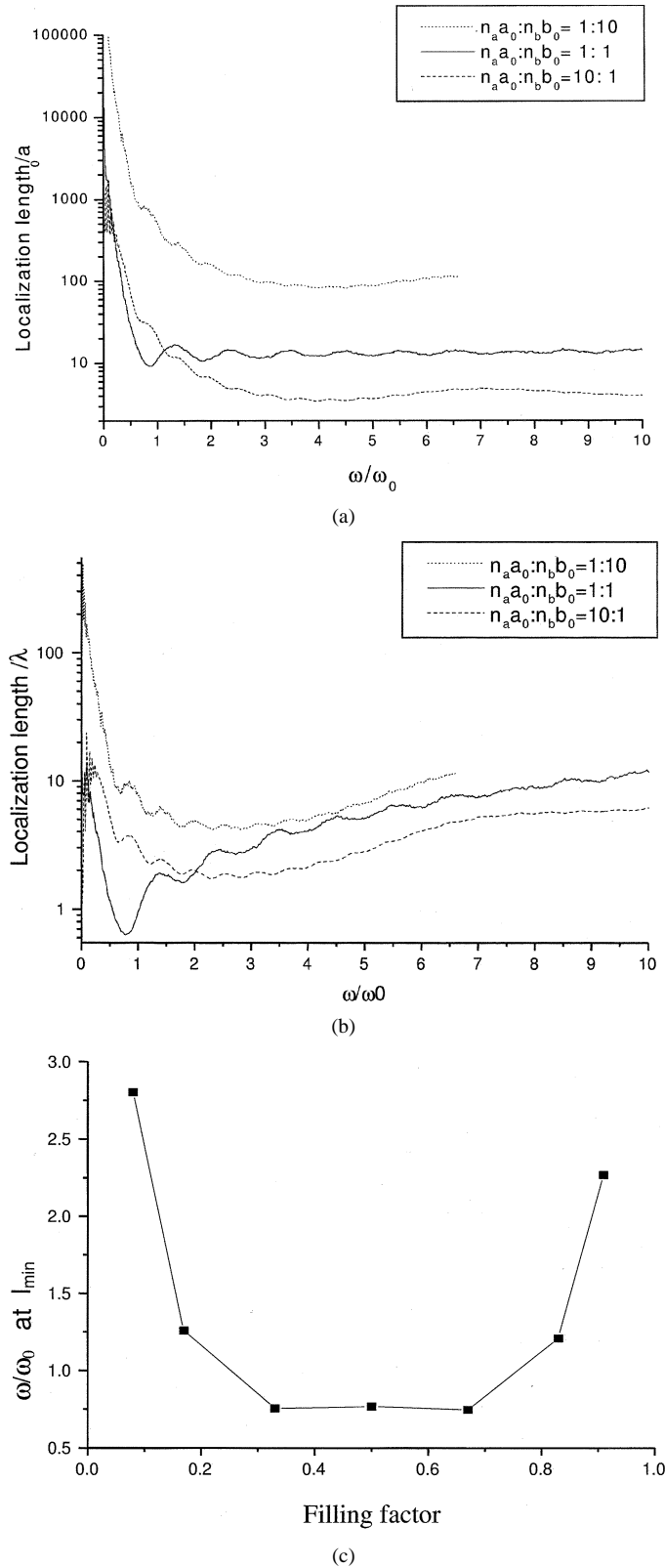
(a)

(b)

(c)

Fig. 7. Random media with different filling factors. The filling factors ($n_a a_0$: $n_b b_0$) are 1:10 for dotted line, 1:1 for solid line, and 10:1 for dashed line. (a) Localization length/a_0 versus ω/ω_0. (b) Localization length/λ versus ω/ω_0. (c) ω at minimum localization versus filling factor.

ensemble-averaged behavior of the random media. To compare with experimental data, it is important to understand the resonant modes in individual samples.
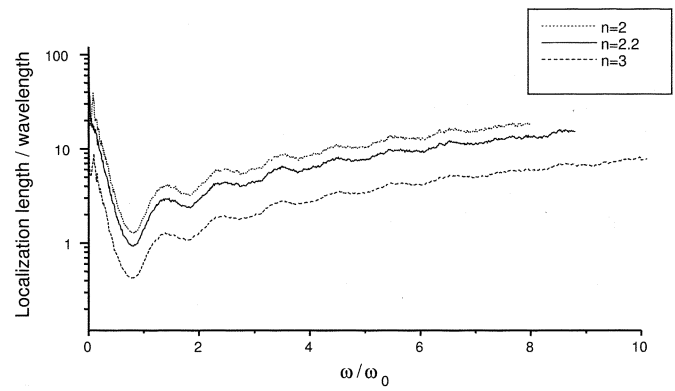

Fig. 8. Localization/λ versus ω/ω_0 for different refractive index. The refractive index is $n = 2$ for the dotted line, $n = 2.2$ for the solid line, and $n = 3$ for the dashed line.

The transmission spectrum of a single sample is plotted in Fig. 9(a). This sample is a completely random system with degree of randomness $\sigma = 0.9$. The sample length is larger than the decay length. Light is localized in this sample. The sharp lines indicate the resonant cavity modes in the sample. The spectral linewidth reflects the quality factor of the random cavity which determines the lasing threshold. By increasing the spectral resolution, the linewidth of the resonant modes could be found in the transmission spectrum. However, when the separation of central frequencies of two resonant modes is smaller than their linewidth, their transmission peaks are overlapped in the transmission spectrum. It is then difficult to separate these two modes to obtain their linewidth.

Thus, we use a different and more efficient method to extract the spectral linewidth of cavity modes. The frequency and linewidth of the resonant mode in a dielectric medium can be found by solving for the eigenmodes of the dielectric system. A resonant mode is an eigenmode of the system. For the periodic structure, in the passband there are $n - 1$ resonant modes corresponding to the $n - 1$ eigenmodes of the n-layer system. Similarly, in the random media, we can find the resonant modes by solving for its eigenmodes.

In a system of finite size, photons in a resonant mode can leak out of the system. This loss gives a nonzero linewidth for the resonant mode. We call these leaky resonant modes quasi-states. In the transfer matrix method, a quasi-state satisfies the boundary conditions that there is no input light into the system, but there may be outgoing wave.

The propagation of light in 1-D random media can be calculated by a transfer matrix $\begin{pmatrix} m_{11} & m_{12} \\ m_{21} & m_{22} \end{pmatrix}$. Input and output light are related by the transfer matrix

$$\begin{pmatrix} p_0 \\ q_0 \end{pmatrix} = \begin{pmatrix} m_{11} & m_{12} \\ m_{21} & m_{22} \end{pmatrix} \begin{pmatrix} p_N \\ q_N \end{pmatrix}. \tag{1}$$

A quasi-mode corresponds to zero input light, e.g., $p_0 = 0$, $q_n = 0$. Therefore, (1) becomes

$$\begin{pmatrix} 0 \\ q_0 \end{pmatrix} = \begin{pmatrix} m_{11} & m_{12} \\ m_{21} & m_{22} \end{pmatrix} \begin{pmatrix} p_N \\ 0 \end{pmatrix}. \tag{2}$$

Fig. 9(b) illustrates the boundary conditions for a quasi-state. Such conditions require $m_{11} = 0$. In order to satisfy $m_{11} = 0$,
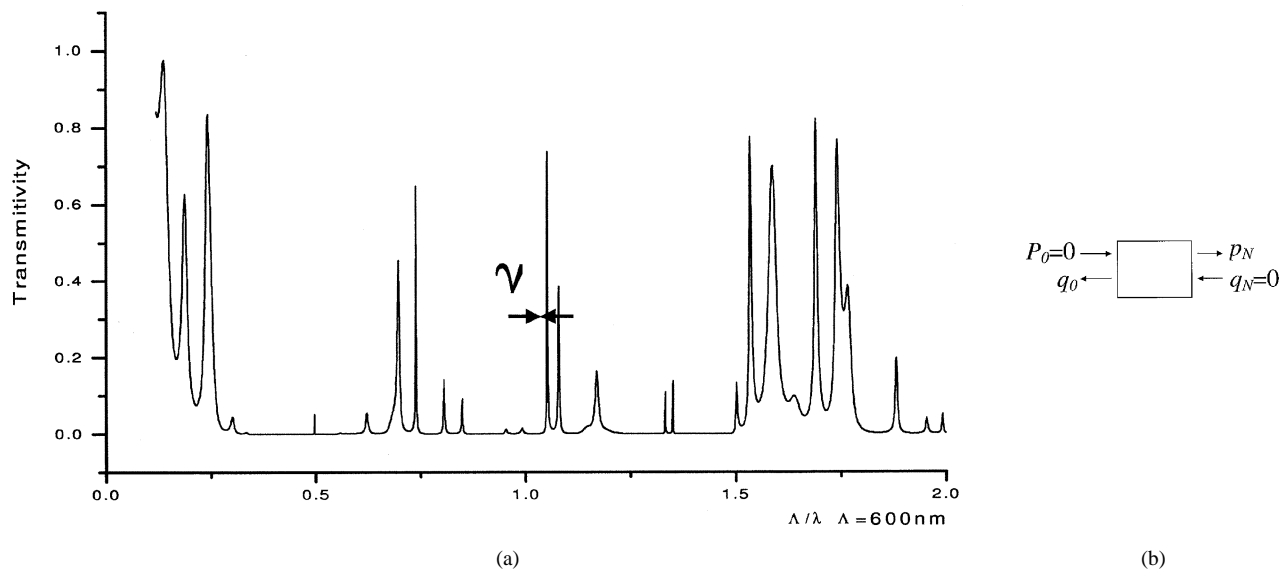
Fig. 9.   (a) Transmission spectrum of a single sample. (b) Quasi-state leaky mode.
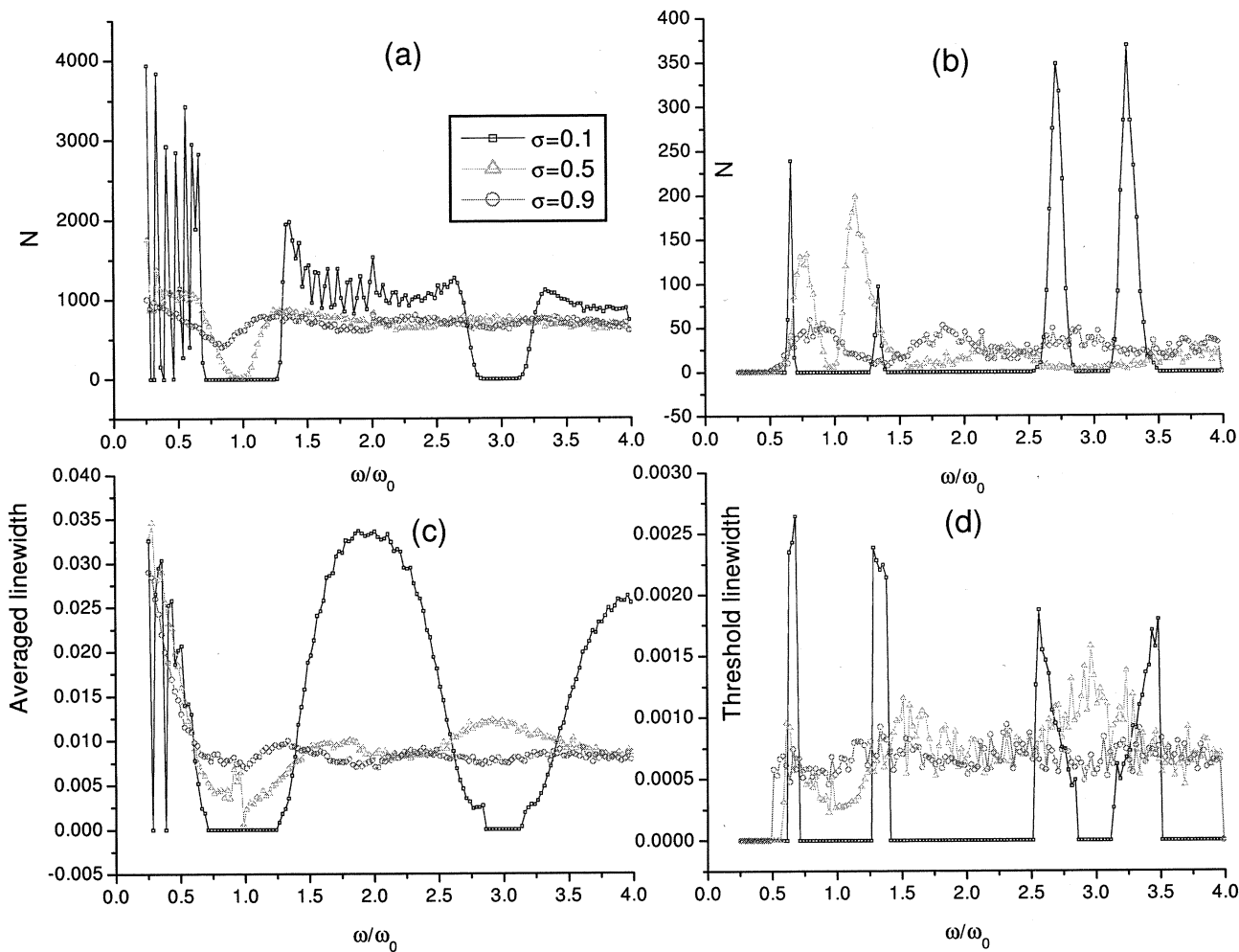

Fig. 10.   Linewidth distribution for first lasing mode [(b) and (d)] and all possible modes (density of state) [(a) and (c)]. (a), (b) Number density versus ω. (c), (d) Mean linewidth versus ω.

the eigenfrequency ω must have an imaginary part. The imaginary part γ of ω corresponds to the linewidth of the quasi-state.

We compared the result of a periodic structure obtained with the above method to the direct calculation of full-width at half maximum (FWHM) of the transmission peaks. There is a
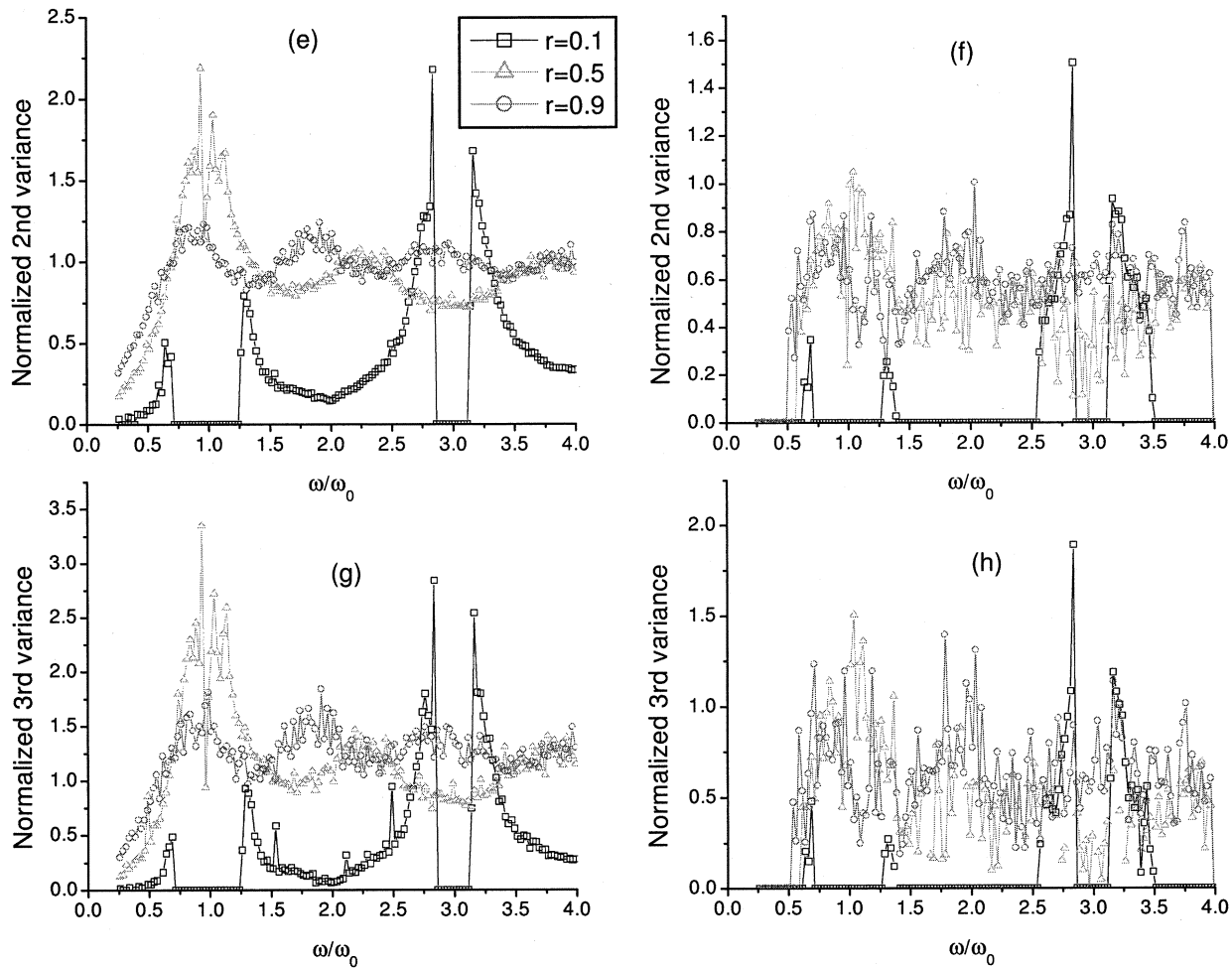
Fig. 10. *(Continued.)* Linewidth distribution for first lasing mode [(f), and (g)] and all possible modes (density of state) [(e), and (f)]. (e), (f) Normalized second-order variance versus ω. (g), (h) Normalized third-order variance versus ω.

one-to-one correspondence of the quasi-states of the system and the transmission peaks of the periodic structure. The linewidth of the quasi-states matches the FWHM of the transmission peaks.

We apply this method to find quasi-states in individual samples. We find that the frequency and the linewidth of quasi-states also match the frequency and the FWHM of the transmission peaks in the transmission spectrum.

To obtain the general behavior of the quasi-states in the random system, in Fig. 10 we plot the ensemble averaged linewidth of the quasi-states in the random system versus frequency. The frequency is normalized to ω_0. The system is a completely random system consisting of ten dielectric layers and nine air gap layers. The refractive index ratio is $n_a a_0 : n_b b_0 = 1 : 1$. We take 4000 random configurations for each value of randomness.

We obtain the density of states from the distribution of all these resonant modes in the 4000 random configurations. In each sample, among all the modes, we pick up the mode with the minimum linewidth (maximum quality factor). This mode has lowest loss and will lase first in this particular sample with increase of optical gain. The statistics of these modes with minimum linewidth (first lasing modes) gives the distribution of lasing threshold of the random system.

In Fig. 10, we plot the statistics of both the first lasing modes and all modes (density of states) versus frequency. In Fig. 10(a) and (b), we plot the distribution of the first lasing modes and the density of states. This plot indicates how the modes are distributed in the frequency domain. In Fig. 10(c) and (d), we plot the mean linewidth of the first lasing modes and all modes versus frequency. In Fig. 10(e) and (f), we plot the normalized second-order variance $\langle (\gamma/\bar{\gamma}) - 1)^2 \rangle$, where $\bar{\gamma}$ is the average linewidth. This plot tells the width of the distribution. In Fig. 10(g) (h), we plot the normalized third-order variance $\langle ((\gamma/\bar{\gamma}) - 1)^3 \rangle$. This value tells whether the linewidth distribution is symmetric with respect to mean linewidth $\bar{\gamma}$. Symmetric distribution gives zero value of normalized third-order variance.

From Fig. 10(b), the first lasing modes are located mostly at the band edge when the randomness is small. As the randomness increases, the lasing mode moves toward the stopband center, the density of states in the passband decreases and the density of states in the stopband increases [see Fig. 10(a)].

From Fig. 10(d) the lasing threshold decreases for the modes located in passband and decreases in the stopband as the randomness increases. In Fig. 10(c), the frequency dependence of the mean linewidth is similar to that of localization length and transmissivity. In the stopband, when the degree of randomness in the system is small, the linewidth is almost zero in center of

the stopband. Only near the band edge, the linewidth has a small value. When the randomness of the system increases, the value of the linewidth increases in the stopband. This means that there is a higher probability of finding a cavity mode inside the stopband and the linewidth increases as the randomness increases in the system.

In the passband, the linewidth is large when the randomness is small. As the randomness of the system increases, the linewidth decreases and the quality of cavity modes increases; i.e., the modes in the passband become less lossy and have a lower lasing threshold. When the randomness is very large, the linewidth of quasi-states is the same across all frequencies. Thus the lasing modes can be found at any frequency.

We also calculate the variance of linewidth of the lasing modes as shown in Fig. 10(e) and (f). The normalized second-order variance gives the fluctuation of lasing threshold. As the randomness of the system increases, the distribution of lasing threshold becomes wider. In the stopband region, the distribution of lasing threshold is wider than that in the passband region when the randomness is small. When the randomness is large, the distribution of lasing threshold is about the same in all frequency regions.

Fig. 10(g) and (h) plot the normalized third-order variance. The third-order variance tells whether the distribution of linewidth is symmetric with respect to the averaged linewidth value. As the randomness increases, the distribution of the lasing threshold becomes less symmetric. The distribution of linewidth for all quasi-states is asymmetric in the stopband, but symmetric in the passband. As the randomness of the system increases, the distribution of the linewidth for all quasi-states becomes more asymmetric.

We compare the linewidth of quasi-states in a random system with the linewidth of the mode near the edge of passband of a periodic structure and the linewidth of a single defect state in a periodic system. The results indicate that the single-defect system has the smallest linewidth when the defect is located in the center of the stopband. But in a highly disordered system, the minimum linewidth of the quasi-states is comparable to that of the single defect mode. The lasing threshold in the highly disordered system can be close to that of the single-defect mode.

In Fig. 11, we plot the lasing threshold versus disorder in the completely random system with filling factor 1:1. The lasing threshold first decreases then increases as the disorderness increases. The minimum lasing threshold occurs not in a perfectly ordered system or completely disordered system, but in a system with certain degree of disorder.

VIII. CONCLUSION

Our calculations for 1-D periodic structures show that there are three types of passbands: particle-related passbands, gap-related passbands, and combined passbands. The particle related passbands originate from the Fabry–Perot resonance of a single particle and the gap-related passbands come from the Fabry–Perot resonance of a single air gap. At common multiples of single-particle and single-gap resonant frequencies, a particle-related passband and a gap-related passband merge and form a combined passband. When randomness is introduced
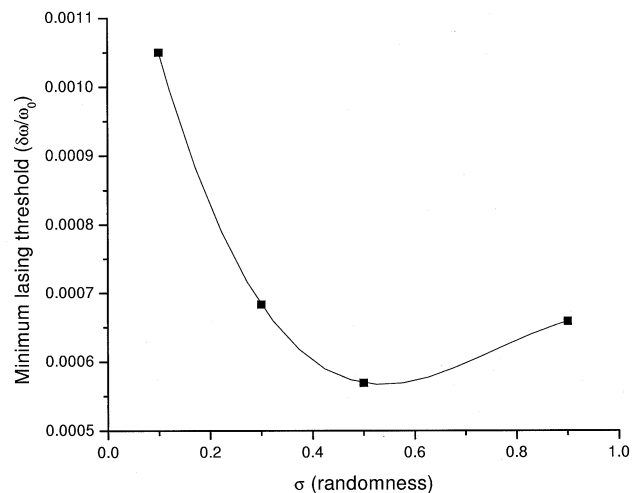

Fig. 11. Minimum lasing threshold versus randomness in the system of completely random system with a 50% filling factor.

to a periodic system, the behavior of a passband depends on its origin. For example, when the spacing between particles is randomized but the particle size remains uniform, the gap-related passbands diminish and eventually disappear at a large degree of disorder. But the particle-related passbands survive and the maximum transmissivity of particle-related passbands remains unity, no matter how large the randomness is. We explain this result with the single-particle resonance. When the particle size is randomized but the particle spacing is kept constant, the particle-related passbands disappear, but the gap-related passbands remain. In both cases, the combined passbands remain. The reason that some passbands survive is that some degree of order remains in the random structure. When both the particle size and spacing are randomized, all three types of passbands diminish and eventually disappear. The complete random medium behaves like a broadband mirror through the entire frequency region.

In such a random system, light can experience high reflection from the multiple dielectric layers of random thickness and random spacing. With two stacks of those multiple layers of high reflectivity which serve as two highly reflective mirrors, light will be confined in between and a resonant cavity is formed. Light inside the random cavity penetrates both sides of the mirrors for certain distance. This penetration length gives the size of the random cavity. This value also determines the number of layers needed to trap the photons inside. We found that the optimal region of strong localization occurs in the sample of 50% filling factor.

We calculate the spectral linewidth and lasing threshold of quasi-states in the 1-D random system. The statistics of all quasi-states gives the frequency dependence of the density of states. In each sample, we pick the mode with the smallest linewidth or highest quality factor. This mode will lase first. The statistics of linewidth of the first lasing modes gives the distribution of the lasing threshold. Both statistics of the lasing threshold and the density of states show strong bandgap effect. In a weakly disordered system, the lasing mode is located near the band edge and the density of states becomes nonzero but small inside the stopband. As the randomness

increases, the first lasing mode moves toward the stopband center and the density of states increases in the stopband. In the highly disordered system, the mean value of the lasing threshold is uniform through the entire frequency region and the distribution of lasing threshold is asymmetric with respect to the mean value of the threshold. The spatial mode profile of the first lasing mode is highly localized in the middle of the sample. The minimum lasing threshold occurs at certain degree of disorder. The results of this paper are restricted to 1-D system. Localization behaviors in higher dimensional systems are dramatically different [24] and deserve further study.

ACKNOWLEDGMENT

REFERENCES

[1] H. Cao, J. Y. Xu, E. W. Seeling, and R. P. H. Chang, "Microlaser made of disordered media," *Appl. Phys. Lett.*, vol. 76, pp. 2997–2999, 2000.
[2] H. Cao, Y. G. Zhao, S. T. Ho, E. W. Seelig, Q. H. Wang, and R. P. H. Chang, "Random laser action in semiconductor powder," *Phys. Rev. Lett.*, vol. 82, pp. 2278–2281, 1999.
[3] H. Cao, J. Y. Xu, Z. Q. Zhang, S. H. Chang, S. T. Ho, E. W. Seelig, X. Liu, and R. P. H. Chang, "Spatial confinement of laser light in active random media," *Phys. Rev. Lett.*, vol. 84, pp. 5584–5587, 2000.
[4] *Scattering and Localization of Classical Waves in Random Media*, P. Sheng, Ed., World Scientific, Singapore, 1990.
[5] S. John, "Localization of light," *Phys. Today*, vol. 44, pp. 32–40, May 1991.
[6] D. S. Wiersma, P. Bartolini, A. Lagendijk, and R. Righini, "Localization of light in a disordered medium," *Nature*, vol. 390, pp. 671–673, 1997.
[7] F. J. P. Schuurmans, D. Vanmaekelbergh, J. Van de Lagemaat, and A. Lagendijk, "Strongly photonic macroporous gallium phosphide networks," *Science*, vol. 284, pp. 141–143, 1999.
[8] S. John, "Strong localization of photons in certain disordered dielectric superlattices," *Phys. Rev. Lett.*, vol. 58, pp. 2486–2489, 1994.
[9] A. R. McGurn, K. T. Christensen, F. M. Mueller, and A. A. Maradudin, "Anderson localization in one-dimensional randomly disordered optical systems that are periodic on average," *Phys. Rev. B*, vol. 47, pp. 13 120–13 125, 1993.
[10] A. Kondilis and P. Tzanetakis, "Light propagation and localization in disordered binary multilayer films: An approximate analytical solution," *J. Opt. Soc. Amer. A*, vol. 11, pp. 1661–1666, 1994.
[11] V. D. Freilikher, B. A. Liansky, I. V. Yurkevich, A. A. Maradudin, and A. R. McGurn, "Enhanced transmission due to disorder," *Phys. Rev. E*, vol. 51, pp. 6301–6304, 1995.
[12] S. A. Bulgakov and M. Nietto-Vesperinas, "Competition of different scattering mechanisms in a one-dimensional random photonic lattice," *J. Opt. Soc. Amer. A*, vol. 13, pp. 500–508, 1996.
[13] L. I. Deych, D. Zaslavsky, and A. A. Lisyansky, "Statistics of the Lyapunov exponent in 1D random periodic-on-average systems," *Phys. Rev. Lett.*, vol. 81, pp. 5390–5393, 1998.
[14] S. A. Bulgakov and M. Nieto-Vesperinas, "Field distribution inside one-dimensional random photonic lattices," *J. Opt. Soc. Amer. A*, vol. 15, pp. 503–510, 1998.
[15] M. Born and E. Wolf, *Principles of Optics*, 7th ed. New York: Cambridge, 1999, sec. 1.6.5.
[16] A. Yariv and P. Yeh, *Optical Waves in Crystal*. New York: Wiley, 1983.
[17] P. Yeh, A. Yariv, and C. Hong, "Electromagnetic propagation in periodic stratified media, I general theory," *J. Opt. Soc. Amer.*, vol. 67, pp. 423–438, 1977.
[18] A. Yariv and P. Yeh, "Electromagnetic propagation in periodic stratified media, II birefringence, phase matching and x-ray lasers," *J. Opt. Soc. Amer.*, vol. 67, pp. 438–448, 1977.
[19] P. Sheng, B. White, Z.-Q. Zhang, and G. Papanicolaou, "Minimum wave-localization length in a one-dimensional random medium," *Phys. Rev. B*, vol. 34, pp. 4757–4761, 1986.
[20] Z.-Q. Zhang, K.-C. Chiu, and D. Zhang, "Method to measure the localization length in one dimension," *Phys. Rev. B*, vol. 54, pp. 11 891–11 894, 1996.
[21] K. M. Leung, "Defect modes in photonics band structures: A Green's function approach using vector Wannier functions," *J. Opt. Soc. Amer. B*, vol. 10, pp. 303–306, 1993.
[22] N. Liu, "Defect modes of stratified dielectric media," *Phys. Rev. B*, vol. 55, pp. 4097–4100, 1997.
[23] D. R. Smith, R. Dalichaouch, N. Kroll, S. Schultz, S. L. McCall, and P. M. Platzman, "Photonic band structure and defects in one and two dimensions," *J. Opt. Soc. Amer. B*, vol. 10, pp. 314–321, 1993.
[24] B. Kramer and A. Mackinnon, "Localization—Theory and experiment," *Rep. Prog. Phys.*, vol. 56, no. 12, pp. 1469–1564, 1993.

Shih-Hui Chang received the B.S. degree in physics from National Taiwan University, Taiwan, R.O.C., in 1994, and the M.S. degree in physics from University of California, Riverside, in 1996. Currently, he is working toward the Ph.D. degree in electrical and computer engineering at Northwestern University, Evanston, IL.

He has been a Research Assistant in the Electrical and Computer Engineering Department, Northwestern University, since 1999. He has published three conference papers and seven journal papers in the area of photonics.

Mr. Chang is a member of the Optical Society of America (OSA).

Hui Cao received the Ph.D. degree in applied physics from Stanford University, Stanford, CA, in 1997.

Currently, she is an Associate Professor in the Department of Physics and Astronomy, Northwestern University, Evanston, IL.

Dr. Cao received Alfred P. Sloan Fellow in 2000, the David and Lucille Packard Fellow in 1999, and the National Science Foundation (NSF) CAREER Award in 2001. She is a member of the Optical Society of America (OSA) and the American Institute of Physics (AIP).

Seong Tiong Ho (M'01) received the B.S., M.S., and Ph.D. degrees from the Massachusetts Institute of Technology (MIT), Cambridge.

From 1981 to 1984, he was a research member in the Laser Gyroscope Research Group of Northrop Corporation, Norwood, MA. From 1984 to 1989, he was a research member in the Optical Communications Research Group of MIT. From 1989 to 1991, he was a Member of Technical Staff in the Solid State and Quantum Physics Research Laboratory, AT&T Bell Laboratories, Murray Hill, NJ. He joined Northwestern University, Evanston, IL, in 1991, where he was an Assistant Professor in the Department of Electrical Engineering and Computer Science from 1991 to 1996. Since April 1997, he has been an Associate Professor, engaged in research in the area of nanophotonics and quantum electronics. His research interests include nanoscale microcavity semiconductor lasers, lasing in random media, quantum phenomena in low-dimensional photonic structures, nanofabrication of optical micro-resonators, nonlinear optical phenomena in semiconductors and organic polymers, femtosecond ultrafast all-optical switching in nonlinear thin-film waveguides, and electrooptic modulators based on erbium-doped BaTiO3 thin films.

Dr. Ho is a Fellow of the Optical Society of America (OSA).